Flight Controller Design and Autonomous Flight Tests of 60cm-sized UAV

Jin Fujinaga *, Hiroshi Tokutake †, and Shigeru Sunada ‡

Osaka Prefecture University, Sakai, Osaka, 599-8531, Japan

This paper describes the design of flight controller for a fixed-wing small-sized UAV and the autonomous flight tests. The UAV which has been developed by the authors has 0.6m span and its weight is 0.27kg. It cruises at 6-12m/s. The flight controller is composed of attitude stability augment systems, feedforward filters, and guidance systems. The flight controller is designed for longitudinal and lateral-directional motions, separately. The UAV has advantages in safety and portability due to its light weight and low cruising speed. In order to ensure robust stability, the attitude stability augment systems are designed for these motions with μ-synthesis. The feedforward filters are designed in order to shape the command from guidance system to the inner closed-loop appropriately. The longitudinal guidance system, which is designed with PID-control manner, keeps the UAV at a desired altitude. The lateral-directional guidance system guides the UAV to the pre-defined waypoints with avoiding known obstacles. It is designed using the Artificial Potential Field Method. These flight controllers are implemented on the small on-board computer we have also developed. Autonomous flight experiments show that the developed UAV is able to fly autonomously, passing over pre-defined waypoints, and that the UAV has the ability of avoiding the known obstacle.

Nomenclature

$A_{\mathrm{obs}}, \varepsilon_{\mathrm{obs}}$	Parameters of the obstacle potential function
g	Acceleration of gravity
K_ϕ, K_γ	The lateral-directional and longitudinal feedforward filter gains
p	Roll rate
q	Pitch rate
r	Yaw rate
$\boldsymbol{r}$	The position of the UAV
$\boldsymbol{r}_{\mathrm{obs}}$	The position of the obstacle
$\boldsymbol{r}_{\mathrm{wp}}$	The position of the waypoint
T_ϕ, T_γ	Time constants of lateral-directional and longitudinal feedforward filters
U_0, u	x-body axis velocity
U_{art}	The artificial potential field
U_{obs}	The obstacle potential field
U_{wp}	The waypoint potential field
x, y	x- and y-position of the UAV
$x_{\mathrm{wp}}, y_{\mathrm{wp}}$	x- and y-position of the waypoint
$x_{\mathrm{obs}}, y_{\mathrm{obs}}$	x- and y-position of the obstacle
$\boldsymbol{x}_{\mathrm{lat}}, \boldsymbol{x}_{\mathrm{lon}}$	State variable
δ_{a}	Aileron deflection realized by deflecting right and left elevons asymmetrically
δ_{ac}	Aileron deflection command output by the lateral-directional feedforward filter
δ_{e}	Elevator deflection realized by deflecting right and left elevons in the same direction
δ_{th}	Thrust command output from the longitudinal feedforward filter

*Graduate Student, Department of Aerospace Engineering, fujinaga@aero.osakafu-u.ac.jp

†Assistant Professor, Department of Aerospace Engineering, tokutake@aero.osakafu-u.ac.jp

‡Associate Professor, Department of Aerospace Engineering, sunada@aero.osakafu-u.ac.jp

ϕ	Bank angle
ϕ_{com}	Bank angle command generated by guidance logic
γ	Path angle
γ_{com}	Path angle command generated by guidance logic
ψ	Heading angle
ψ_d	Desired heading angle

I. Introduction

Recently, unmanned aerial vehicles (UAVs) have become employed in increasingly important roles. Their autonomous operation has been progressively developed for practical applications in both military and commercial areas. Most of UAVs developed until now are larger than 1 meter and heavier than 1 kg. However, small UAVs are thought to have many advantages such as portability and safety. And when we come to think of missions in urban area or short range missions, it is thought that small and light UAVs are suitable for such missions. The recent developments of efficient small motors, miniature sensors, servo motors, inexpensive micro-computers and GPS navigation systems enable us to develop small-sized UAVs at a low cost. However, smaller and lighter UAVs are generally sensitive to gusts of wind. In addition, sensor noises and model uncertainties make the UAV's performance worse. As a consequence, the flight controller should be designed with sufficiently robust stabilities. There exist many studies investigating flight control and guidance system.[1–3] We design the attitude stability augment system using μ-synthesis.[4,5] To achieve required missions efficiently, the flight controller should guide the UAV with a suitable guidance method. In addition, when the UAV becomes aware of obstacles, the UAV should perform the missions with avoiding the obstacles. The guidance system design is widely studied as the "2-D guidance problem".[6–10] We deal with the obstacle avoidance problem using the artificial potential field method.[11]

This paper describes the flight controller design that ensures robust stabilities and performances and that guides the UAV to pre-defined waypoints with avoiding a known obstacle. Flight tests results are also described. First, in Section II, the developed UAV's airframe, physical characteristics, avionics, aerodynamics measured through wind tunnel experiments, and overall systems are described. Then, in Section III, a flight controller design procedure is discussed. Then, in Section IV, a numerical simulation is performed and the effectiveness of the designed flight controller is discussed. Especially, the numerical simulation for the guidance system is performed. Finally, in Section V, the result of an autonomous flight test with avoiding a known obstacle is described.

II. Description of the developed UAV

A. Airframe

Figure 1 shows an overview of the developed UAV. Our UAV's components are mainly made of styrene foam due to the ease of processing this material and its lightness. The baseline airframe was selected for its compactness and wing loading value. Our UAV has the following physical characteristics:

- Wing
  - Span : 0.6 m
  - Aspect ratio : 2.67
  - Airfoil : CLARK-YS
  - Tip chord : 0.15 m
- Weight(no payload) : 0.27 kg
- Velocity : 6-12 m/s
- Thrust : propeller driven by a brushless motor
- Control surface : elevons actuated by servo motors
- Battery : Lithium-Polymer (11.1 Voltage, 450mAh, and 0.035 kg)
- Endurance : approximately 15 minutes at 6.5 m/s

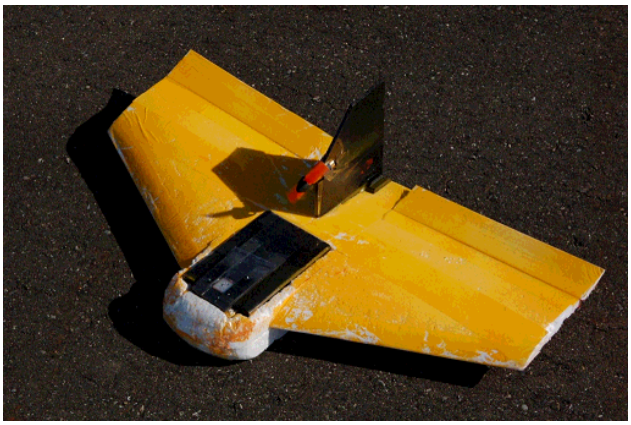

Figure 1. Overview of the developed UAV.

B. Avionics

The avionics system is a major weight component for a small UAV. Even if an airframe is small, the sensors and flight computer must have the same functions as those for a larger UAV. In addition, the flight control system plays a pivotal role in gust reduction for a small UAV, which is accomplished using higher-order controllers based on advanced control methods. Furthermore, a flexible programming approach is required for the implementation and adjustment of controllers. From these requirements, our research group and a cooperating company (Y's Lab INC.) have developed general-purpose flight control hardware. This hardware comprises a small, light-weight circuit board, named MAVC1 (Micro Aerial Vehicle Controller 1) of size 75 mm $\times$ 55 mm, and weight 29 g (Fig. 2).

Table 1 shows the functions of the developed board. The board is equipped with accelerometers and rate gyros, and many other devices can be connected. The middleware, which enables communication with connected devices and real-time programming, has also been prepared.

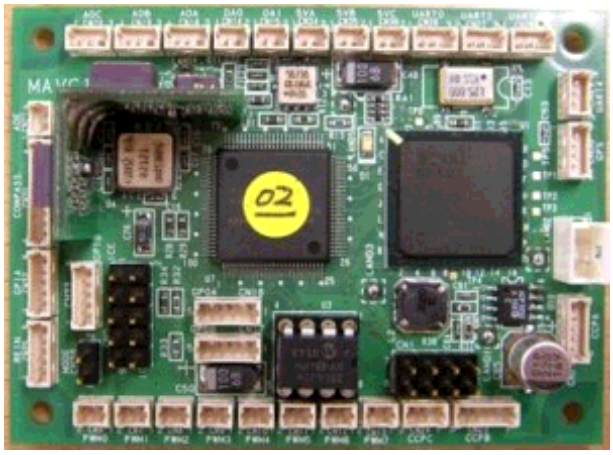

Figure 2. MAVC1 (Micro Aerial Vehicle Controller 1).

C. Overall systems

The designed flight controller is implemented in the MAVC1, while a barometric altimeter,a GPS receiver, a geomagnetism sensor, servo-motors and a brushless motor are connected to it (Fig. 3).

Table 1. Functions of MAVC1.

Computer	Hitachi, HD64F3069
FPGA	Xilinx, XC2S200FG256
Rate gyro	Analog Devices, ADXRS300×3
Accelerometer	Analog Devices, ADXL210JE×2
EEPROM	32Kbite
A/D	6ch
D/A	2ch
Pulse input	10ch
PWM output	8ch
I/O	8ch
UART	4ch
GPS input	1ch
Geomagnetism sensor input	1ch
Rotary encoder input	1ch
5V output	3ch

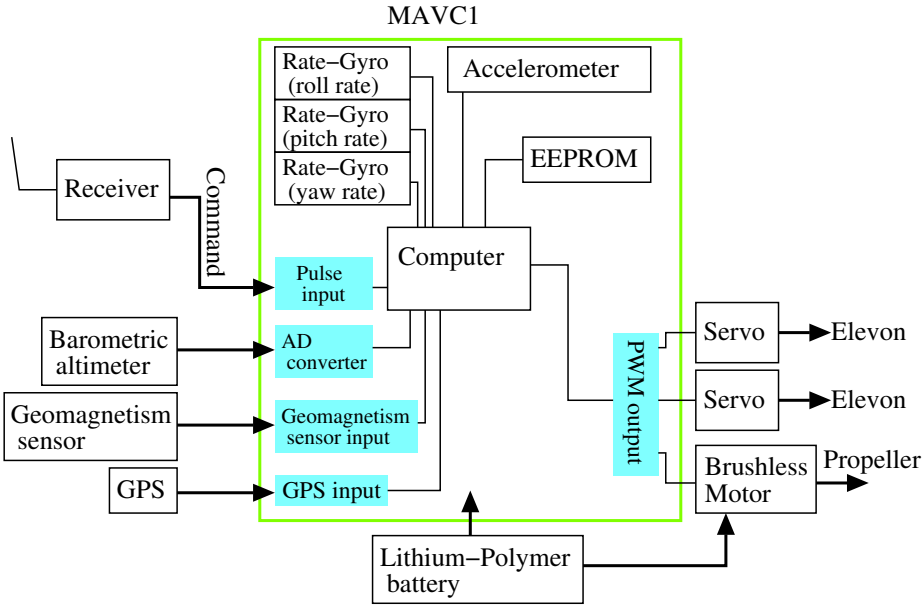

Figure 3. Signal flow.

III. Design of Flight Controller

A. Attitude Stability Augment Systems synthesis

Because the developed UAV is inherently unstable, the stability augment system is essential. It also enhances flight performances.

First, through the wind tunnel experiment, aerodynamic characteristic data was taken. Then, linearized equations of dynamics were identified at selected trim points.[12] The estimated numerical model generally includes uncertainties in the aerodynamic derivatives. In addition, there are several disturbances, for example gusts or sensor noises, in the environment where the UAV will have to fly. In order to treat these problems appropriately, the attitude stability augment system is designed with μ-synthesis.[4,5] Longitudinal and lateral-directional motions are treated separately. The longitudinal attitude stability augment system senses pitch rate and thrust command, then outputs elevator deflection command. The lateral-directional attitude stability augment system senses roll and yaw rate, then outputs aileron deflection command.

Through several numerical simulations and several flight tests, it have been shown that the designed attitude stability augment systems work effectively.[13]

B. Feedforward Filter

The feedforward filters are designed in order to process the command from the guidance system appropriately. The longitudinal guidance system outputs the path angle command and the lateral-directional guidance system outputs the bank angle command. If the feedforward filter is the inverse system of the inner closed-loop, the UAV will follow the path angle command or the bank angle command perfectly. However, the closed-loops generally are very high order systems. So, inverse systems would be also high order systems. In addition, if the inner closed-loop has unstable zeros, the inverse system will become unstable.

Therefore, the feedforward filters were designed as follows.
First, as shown in Figs. 4 and 5, the path angle and bank angle responses to the thrust step input and the aileron step input are investigated through numerical simulations, respectively. Then a reciprocal number of the path angle steady value is set as the gain of the first-order lag feedforward filter for the longitude. And a reciprocal number of the bank angle steady value is set as the gain of first-order lag feedforward filter for the lateral-direction. Time constant of the feedforward filter for the longitude is designed as $T_\gamma = 1.5$ sec and for lateral-direction is $T_\phi = 0.5$ sec in order to avoid the impulsive inputs to the inner-loops. With

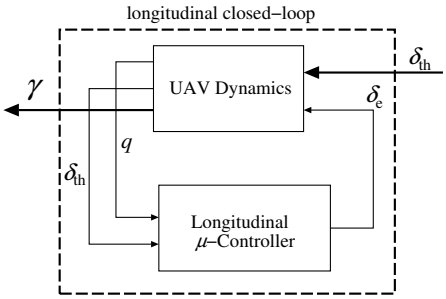

Figure 4. Longitudinal closed-loop

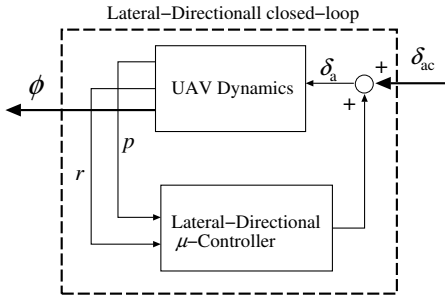

Figure 5. Lateral-directional closed-loop

these feedforward filters, it is expected that the path and bank angle will follow the path and bank angle command well in a low frequency band.

C. Guidance System

Attitude stability augment systems designed with μ-synthesis guarantee robust stability and performance of the inner closed-loop which consists of the UAV dynamics and attitude stability augment systems. Generally, the controller solved with μ-synthesis is very high order system and therefore the closed-loop becomes also high order system. If the guidance system is designed for this high order closed-loop, it may become very complicated and hard to handle. In addition, the closed-loop constructed with the nominal equations of UAV dynamics and μ-controller may not precisely reflect actual closed-loop responses. For these reasons, the inner closed-loop dynamics were identified as a low-order model through several flight tests, and the

guidance system was designed for the low-order model. Actual responses to a thrust step input for longitude or an aileron step input for the lateral-direction were measured. The identified closed-loop was expressed in a simple form such as a first-order lag or a integral form (Figs. 6, 7).

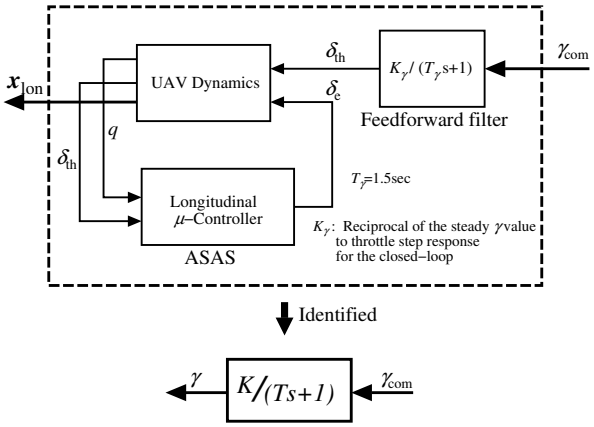

Figure 6. Closed-loop with path angle command.

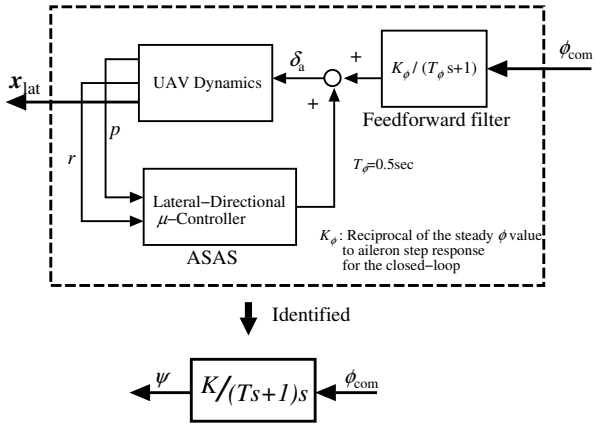

Figure 7. Closed-loop with bank angle command.

As shown in Figs. 6 and 7, the inputs of the identified inner closed-loop are the path angle command for the longitude, and the bank angle command for the lateral-direction. The outputs are the path angle for the longitude, and the yaw angle for the lateral-direction.

1. Longitudinal guidance system

The longitudinal guidance system's goal is to take the altitude close to the desired value. For longitudinal guidance system, the error between the pre-defined altitude and the current UAV altitude is the input to the guidance system. The longitudinal guidance system is designed for the simplified inner closed-loop with Proportion, Integral, and Derivative (PID) control manner (Fig. 8). The PID controller gains were tuned suitably through trial-and-error.

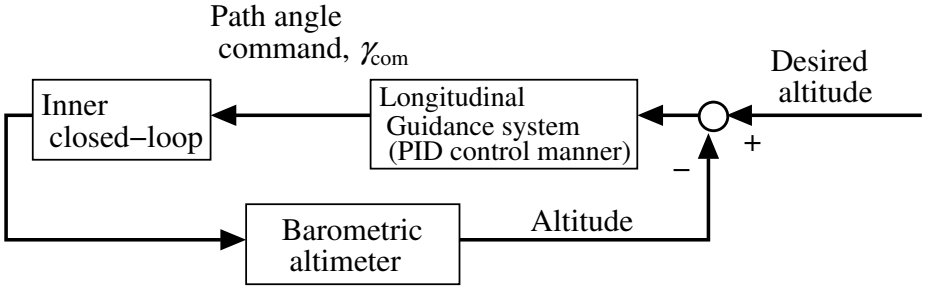

Figure 8. Longitudinal guidance logic

2. Lateral-directional guidance system

The lateral-directional guidance system's goal is to take the UAV close to the waypoint. To lead the UAV to the pre-defined waypoint with avoiding known obstacles, the potential field method was used. The potential field method has been widely used as a tool for path planning in the robotics community. As shown in Fig. 9, the ψ_d is calculated with the potential field method and the error between ψ_d and the current UAV heading angle is compensated with PID control manner.

The obstacle avoidance problem of the UAV with a single obstacle was treated. $\boldsymbol{r}_{\rm wp}$ denotes the waypoint position and $\boldsymbol{r}_{\rm obs}$ denotes the obstacle position. It is assumed that the waypoints are pre-defined and the position of a obstacle is known. The desired heading angle command, ψ_d, is calculated using the artificial

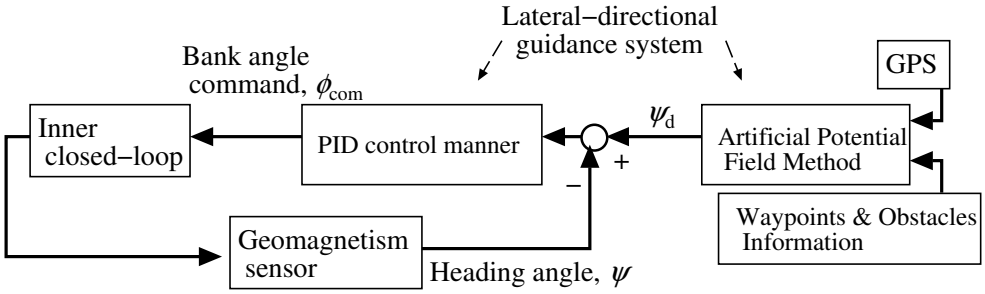

Figure 9. Lateral-directional guidance logic

potential field, $U_{\rm art}(\boldsymbol{r})$, by

$$\psi_d = \tan^{-1}\left(\frac{\partial U_{\rm art}(\boldsymbol{r})/\partial x}{\partial U_{\rm art}(\boldsymbol{r})/\partial y}\right).$$

If the UAV's heading converges the desired heading angle well, it is expected that the UAV will reach a local minimum point. The artificial potential field is expressed as the sum of attractive potential fields, $U_{\rm wp}$, and repulsive potential fields, $U_{\rm obs}$.

$$U_{\rm art} = U_{\rm wp} + U_{\rm obs}$$

A pre-defined waypoint is expressed as an attractive potential field whose minimum point is the waypoint. We set the attractive potential field, $U_{\rm wp}(\boldsymbol{r})$, as follows (Fig. 10);

$$U_{\rm wp}(\boldsymbol{r}) = \|\boldsymbol{r} - \boldsymbol{r}_{\rm wp}\| = \sqrt{(x - x_{\rm wp})^2 + (y - y_{\rm wp})^2}.$$

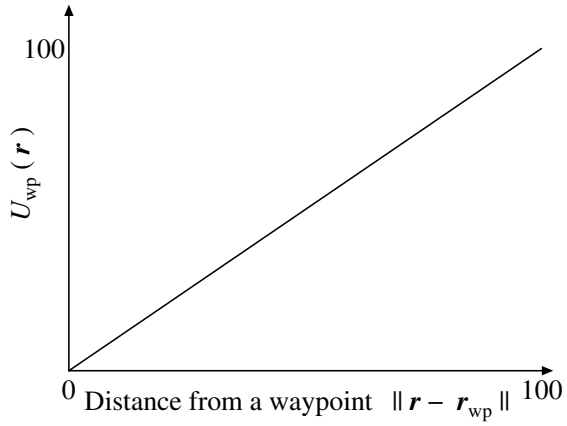

Figure 10. The potential field of the waypoint

A single point obstacle is expressed as a repulsive potential field. The repulsive potential field should be designed to force the UAV to go away from the obstacle point. The repulsive potential field value should tend to be larger as the UAV position approaches the obstacle point. We set the single point obstacle potential field (Fig. 11), $U_{\rm obs}(\boldsymbol{r})$, as

$$U_{\rm obs}(\boldsymbol{r}) = \frac{A_{\rm obs}}{\|\boldsymbol{r} - \boldsymbol{r}_{\rm obs}\|^2 + \varepsilon_{\rm obs}} = \frac{A_{\rm obs}}{(x - x_{\rm obs})^2 + (y - y_{\rm obs})^2 + \varepsilon_{\rm obs}}.$$

The $A_{\rm obs}, \varepsilon_{\rm obs}$ are designing parameters. A non-zero $\varepsilon_{\rm obs}$ plays the role of avoiding "divide by zero".

The PID controller gains that compensate the error between the desired heading angle, ψ_d and the current heading angle, ψ are tuned through numerical simulations and flight tests.

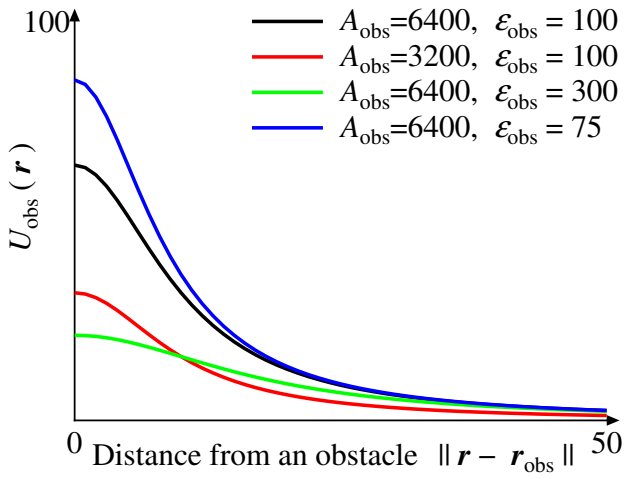

Figure 11. The potential field of the obstacle

IV. Numerical Examples and Simulations

In order to validate the designed flight controller, the numerical simulations were carried out. In this section, the UAV altitude is assumed to be kept at a constant value. The 2-D guidance problem, especially the obstacle avoidance problem is considered. The UAV dynamics can be expressed as follows;

$$\begin{aligned}\dot{x} &= U_0 \sin\psi,\\ \dot{y} &= U_0 \cos\psi,\\ \ddot{\psi} &= -0.83\dot{\psi} + 0.67\phi_{\rm com},\end{aligned}$$

where the velocity of the UAV, U_0, is 8.2 m/s. The PID-control gains from heading error, $\psi_d - \psi$, to bank angle command, $\phi_{\rm com}$, were tuned suitably.

Two waypoints were set as $(x,y)_{\rm wp.1} = (0,0)$, $(x,y)_{\rm wp.2} = (200,0)$. The UAV is required to fly over the 30-meter square zone of these waypoints with/without an obstacle. The obstacle was set as $\boldsymbol{r}_{\rm obs} = (x,y)_{\rm obs} = (100,0)$. The obstacle potential field was assumed as

$$U_{\rm obs}(\boldsymbol{r}) = \frac{6400}{\|\boldsymbol{r} - \boldsymbol{r}_{\rm obs}\|^2 + 100}.$$

In order to confirm the effectiveness of the obstacle avoidance method using the artificial potential field, the numerical simulation results with and without the obstacle were compared. Figure 12 shows the results of the numerical simulation. Both simulation results show that the UAV passes the two waypoints. It can be seen that the UAV goes away from the obstacle when the obstacle was considered, and that this obstacle potential field forces the UAV away from areas within about 20-meters of the obstacle point.

These numerical simulations show that the known obstacles can be avoided using the potential field method.

V. Flight test results

To confirm the effectiveness of the designed flight controller works effectively, the following flight tests were performed. First, four waypoints and a obstacle were set as shown in Fig. 13. The UAV was required to fly over the 30-meter square zone of the waypoints with avoiding the obstacle. The altitude was maintained close to prescribed values. The following function was used as the obstacle potential field;

$$U_{\rm obs} = \frac{6400}{(x+20)^2 + (y+20)^2 + 100}.$$

Figure 14 shows the flight trajectory. It can be seen that the position of the UAV was controlled, passing through the given waypoints. In addition, it is found that the UAV flew with avoiding the obstacle.

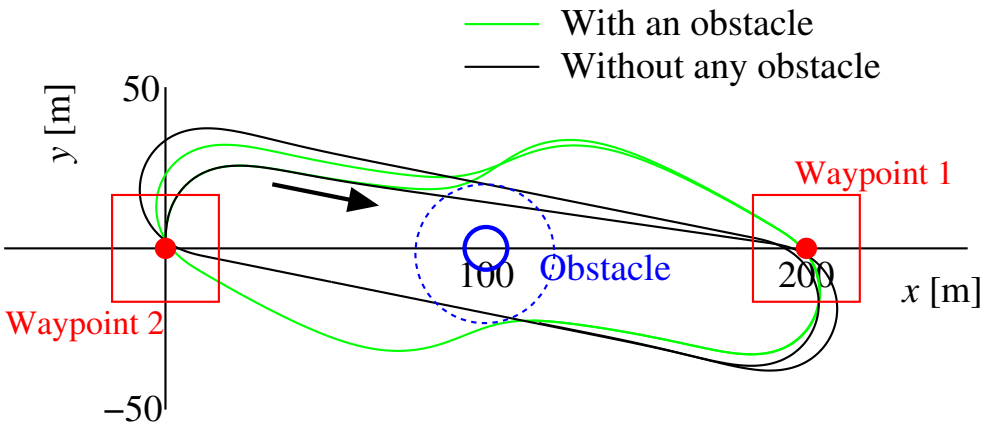

Figure 12. Results of the numerical simulation

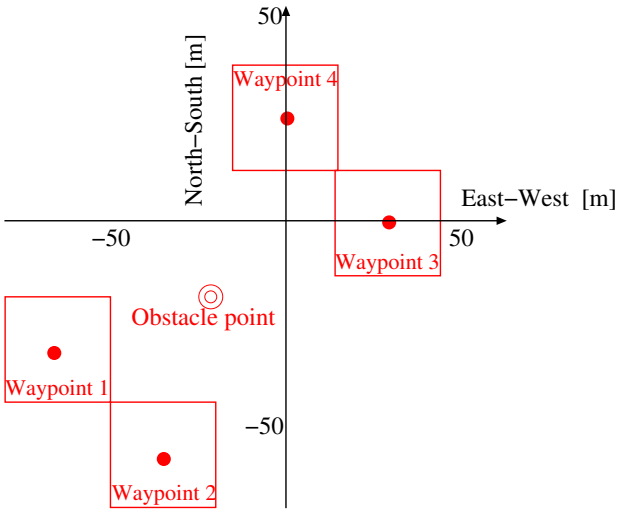

Figure 13. Location of the waypoints and the obstacle

Waypoint No.	x-position, m	y-position, m
1	-65	-35
2	-35	-65
3	30	0
4	0	30
Obstacle point	-20	-20

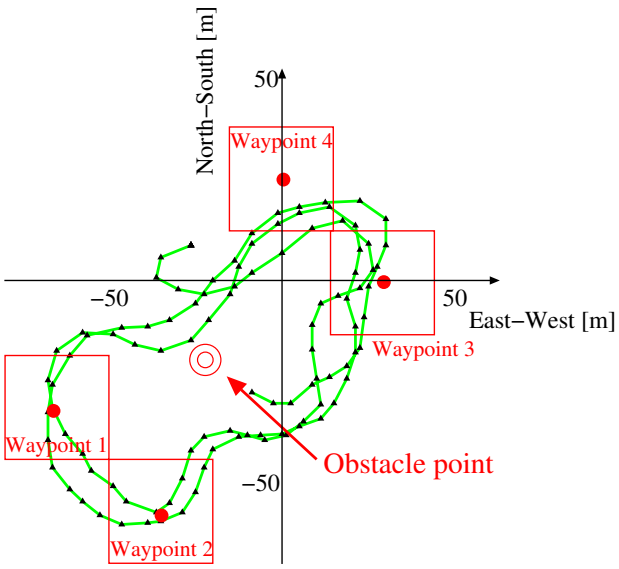

Figure 14. Flight trajectory

VI. Conclusion

The 60-cm sized UAV has been developed. The flight controller, which is composed of the attitude stability augment system, the feedforward filter, and the guidance system, was designed. Because the developed UAV is small and light, the attitude stability augment system was designed using μ-synthesis and robust stabilities and performances were ensured. The feedforward filter was designed in order to process commands from the guidance system appropriately. The longitudinal guidance system was designed in order to keep the UAV at a desired altitude. The lateral-directional guidance system was designed in order to guide the UAV to pre-defined waypoints with avoiding known obstacles. The artificial potential field method was used in the guidance system. The numerical simulations and the flight tests were carried out and it was found that the designed flight controller works effectively and the developed UAV is able to fly autonomously with avoiding the known obstacle.

Acknowledgment

The research was supported in part by the Ministry of Education, Culture, Sports, Science and Technology through a Grant-in-Aid for Scientific Research (S), 18100002, 2006.

References

[1]Jung Soon Jang and Claire J. Tomlin, *Autopilot Design For The Stanford DragonFly UAV: Validation Through Hardware-Ih-The-Loop Simulation*, AIAA Guidance, Navigation, and Control Conference and Exhibit 6-9 August 2001.

[2]Yasmina Bestaoui, Salim Hima, and Chouki Sentouth, *Motion Planning of A Fully Actuated Unmanned Aerial Vehicle*, AIAA Guidance, Navigation, and Control Conference and Exhibit 11-14 August 2003.

[3]Y. Ochi, K. Itoh, and K. Kanai, *Application of H-infinity Control to Missile Guidance and Control*, AIAA Guidance, Navigation, and Control Conference and Exhibit 14-17 August 2000.

[4]Gary J. Balas, John C. Doyle, Keith Glover, Andy Packard, and Roy Smith, *μ-Analysis and Synthesis Toolbox*, MUSYN Inc. and The MathWorks, Inc., 1997.

[5]Kemin Zhou, John C. Doyle, and Keith Glover, *Robust and Optimal Control*, Prentice Hall, 1995.

[6]Rolf Rysdyk, "Unmanned Aerial Vehicle Path Following for Target Observation in Wind", Journal of Guidance, Control, and Dynamics, Vol. 29, No. 5, September-October 2006, pp.1092-pp.1100.

[7]Sanghyuk Park, John Deyst, and Jonathan P. How, "A New Nonlinear Guidance Logic for Trajectory Tracking", AIAA Paper 2004-4900

[8]Karin Sigurd and Jonathan How, "UAV Trajectory Design Using Total Field Collision Avoidance", AIAA Paper 2003-5728

[9]William J. Pisano, Dale A. Lawrence, and Peter C. Gray, "Autonomous UAV Control Using a 3-Sensor Autopilot", AIAA Paper 2007-2756

[10]Derek R. Nelson, D. Blake Barber, Timothy W. McLain, and Randal W. Beard, "Vector Field Path Following for Small Unmanned Air Vehicles", IEEE American control conference 2006

[11]Oussama Khatib, "Real-Time Obstacle Avoidance for Manipulators and Mobile Robots", In Proceedings of the IEEE International Conference on Robotics and Automation, volume 2, pages 500-505,1985.

[12]Etkin, *Dynamics of Flight*, John Wiley & Sons, Inc., 1959.

[13]J. Fujinaga, H. Tokutake, and S. Sunada, " Development of Small Unmanned Aerial Vehicle and Flight Controller Design", AIAA Atmospheric Flight Mechanics Conference and Exhibit 20-23 August 2007.